Hindawi Publishing Corporation
Journal of Nanomaterials
Volume 2013, Article ID 297676, 8 pages
http://dx.doi.org/10.1155/2013/297676

Research Article

Preparation, Characterization, and Mechanistic Understanding of Pd-Decorated ZnO Nanowires for Ethanol Sensing

Xiao Deng,[1,2,3] Shengbo Sang,[1,2] Pengwei Li,[1,2] Gang Li,[1,2] Fanqin Gao,[1,2] Yongjiao Sun,[1,2] Wendong Zhang,[1,2] and Jie Hu[1,2]

[1] *MicroNano System Research Center, College of Information Engineering, Taiyuan University of Technology, Taiyuan, Shanxi 030024, China*
[2] *Key Lab of Advanced Transducers and Intelligent Control System of the Ministry of Education, Taiyuan University of Technology, Taiyuan, Shanxi 030024, China*
[3] *College of Physics and Optoelectronics, Taiyuan University of Technology, Taiyuan, Shanxi 030024, China*

Correspondence should be addressed to Wendong Zhang; wdzhang@tyut.edu.cn and Jie Hu; hujie@tyut.edu.cn

Received 5 October 2013; Accepted 2 December 2013

Academic Editor: Sheng-Rui Jian

ZnO nanowires (ZnO-NWs) and Pd-decorated ZnO nanowires (Pd-ZnO-NWs) were prepared by hydrothermal growth and characterized by scanning electron microscopy (SEM) and X-ray diffraction (XRD). When used for gas sensing, both types of nanowires showed a good selectivity to ethanol but a higher sensitivity and lower operating temperature were found with Pd-ZnO-NWs sensors comparing to those of ZnO-NWs sensor. When exposed to 200 ppm ethanol, our ZnO-NWs sensor showed a sensitivity of about 2.69 at 425°C whereas 1.3 at. % Pd-ZnO-NWs sensor provided a 57% more detection sensibility at 325°C. In addition, both response and recovery times of Pd-ZnO-NWs sensors were significantly reduced (9 s) comparing to the ZnO-NWs. Finally, Pd-ZnO-NWs sensor also showed a much lower detection limit of about 1 ppm. The sensing mechanism of Pd-ZnO-NWs sensors has also been clarified, thereby providing a new perspective for further improvement of the sensing performance of ethanol sensors.

1. Introduction

Semiconducting metal oxides are widely used in environmental monitoring, industrial safety monitoring and medical diagnosis [1–3]. Among different types of metal oxides, zinc oxide (ZnO) is of great interest because of its versatile suitability for a large variety of applications. For example, it can be used in gas sensors [4], solar cells [5], field-effect transistors [6], photodetectors [7], and photocatalysts [8]. In particular, ZnO can be used in toxic [2] and combustible [9] gas sensors.

Comparing to the bulk material, micro- and nanostructured ZnO can provide a much improved performance for device applications [10]. Recently, efforts have been devoted to the realization of gas sensor using ZnO thin films [11], nanoparticles [12], and nanowires [13]. Among them, ZnO-NWs are regarded as the most promising candidate for high sensitivity gas sensors for their higher specific surface area and larger length-to-diameter ratio [14]. It has also been shown that surface decoration of ZnO with noble metal elements such as Pd, Ag, Pt, and Au can largely improve the sensitivity of the device because of the modification of the energy band gap and the increase of the carrier concentration [15–19]. Pd, for example, is one of the most versatile catalytic materials for its excellent oxidation capability of converting hydrocarbons at lower temperature [20]. Hsueh et al. reported that the response of Pd-ZnO-NWs can be increased from 1.56 to 2.60 when exposed to 500 ppm ethanol at 230°C, with a response of a few seconds and a recovery time of more than 100 seconds, respectively [21]. Roy et al. also investigated the Pd-sensitized ZnO nanorods for ethanol sensing, the results show that the response magnitude, response and recovery time are 94%, 14 s and 70 s, respectively, when exposed to 1530 ppm ethanol (in air) at an optimum operating temperature of 200°C [22]. Note that despite the significant

improvement in sensitivity, there are still large challenge for improvement of the recovery time and the detection limit of these ZnO ethanol sensors.

In this work, we studied the sensing performance of ZnO-NWs with or without Pd decoration. Vertical ZnO-NWs with an average diameter of 80 nm and a length of 5 μm were prepared by hydrothermal growth. To investigate the detection sensitivities of ZnO-NWs and Pd-ZnO-NWs, Pd nanoparticles with various concentrations were deposited on the surface of ZnO-NWs. The results show that ZnO-NWs and Pd-ZnO-NWs can have the highest responses and gas selectivity to ethanol at different operating temperatures. Comparing to the ZnO-NWs sensor, Pd-ZnO-NWs (1.3 at. %) sensor showed a much improved sensitivity and response-recovery time to ethanol.

2. Experiment

2.1. Preparation of ZnO-NWs. Vertically aligned ZnO-NWs arrays were grown on glass substrate by two-step hydrothermal method as previously reported [25]. Firstly, 0.2 mM ZnAc ($Zn(CH_3CO_2)_2$, 99.99%, Sigma-Aldrich) was dissolved in 40 mL of ethanol (C_2H_5OH, 99.8%, Guangfu) solution to form a seed solution, which was uniformly dropped on the substrate. Afterwards, the glass sheet was put into an ethanol solution for rinsing for 10 seconds, and the sample was placed on a hot plate for 30 minutes at 300°C. The above process was repeated several times to form a seed layer. Secondly, a growth solution was prepared by dissolving 10 mM zinc nitrate ($Zn(NO_3)_2{\cdot}6H_2O$, 99.0%, Sigma-Aldrich) and 5 mM HMTA ($C_6H_{12}N_4$, 99.5%, Sigma-Aldrich) in 400 mL deionized water with magnetical stirring for 30 minutes and then gradually adding 18.8 mL of ammonia (NH_4OH, 28.0%, Sigma-Aldrich) until the end of preparation. Next, the glass sheet with the pretreated ZnO seed layer facing downward was immersed in the growth solution for 8 hours at 90°C. Finally, the glass sheet was washed with deionized water and dried in nitrogen.

To obtain Pd-ZnO-NWs, the ZnO-NWs were dipped in an ethanol solution of 9.6 mM palladium chloride ($PdCl_2$, 99.9%, Sigma-Aldrich) for 8 s and then dried using an air gun. The cycle was repeated several times. The Pd-ZnO-NWs were annealed at 500°C for 1 hour and then cooled down to room temperature. To improve the stability and the repeatability of the gas sensors, samples of ZnO-NWs and Pd-ZnO-NWs were aged at 200°C for 10 days. Finally, a conductive silver paste was uniformly coated on the sample to form electrodes to ensure the electrical contact between the nanowires and probes.

2.2. Characterization Methods. The morphology of ZnO-NWs and Pd-ZnO-NWs was observed using scanning electron microscope (SEM, Hitachi S-3400N), equipped with X-ray energy dispersive spectroscope (EDS, Bruker). The crystal structure and components of samples were characterized by X-ray diffraction technique (XRD, DRIGC-Y 2000A) with Cu Kα radiation (λ = 0.15406 nm) at 30 kV.

The gas sensing properties of the fabricated sensors were tested using the intelligent analysis system (CGS-1TP, Beijing Elite Tech Co., Ltd, China). Figure 1 shows the schematic of the gas sensitivity analysis system. The gas sensor is fixed on the heated platform until the resistance of the sensor is stable. Then the target gas is injected into the testing chamber (with a testing volume of 18 L) by a microinjector, and two rotating fans in the testing chamber make the gas mixed homogeneously. After the resistance of the sensor reaches a new stable value, the testing chamber is opened to refill air. The response and recovery times are defined as the time needed for 90% of total resistance change after the sensor exposed to the testing gas and to the air, respectively.

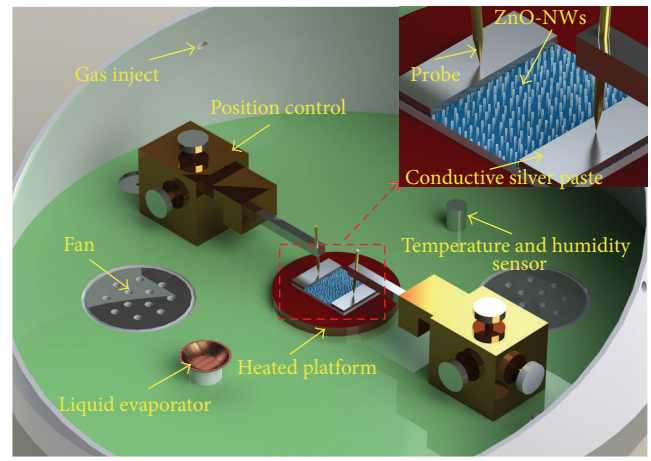

Figure 1: Schematic illustration of a set-up for gas sensitivity analyses. The insert shows a typical device configuration of ZnO-NWs sensor.

The target gas at different concentrations was prepared by a static state method. The whole process of gas dilution could be approximately considered as an isobaric process, resulting in the following relationship between the volume of injected liquid, and the concentration of target gas [26]:

$$V_{\text{liquid}} = \frac{V_s C_{\text{gas}} M}{22.4 \rho d} \times 10^{-9}, \quad (1)$$

where V_{liquid} is the volume of injected liquid, V_s is the volume of testing chamber, C_{gas} is the concentration of target gas, M is the molecular weight of liquid, ρ is the density of liquid, and d is the purity of liquid.

Considering the n-type semiconductor characteristic of ZnO, the response value of gas sensor to reductive gas can be defined as $S = R_a/R_g$, where R_a and R_g are the resistance of sensor in air and in target gas, respectively.

3. Results and Discussion

3.1. Structural Characterization. Figures 2(a) and 2(b) show the top-view and side-view SEM images of ZnO-NWs. It can be observed that the ZnO-NWs vertically grown on the substrate are well aligned. The diameter and length of the nanowires are, respectively, about 70–100 nm and 5 μm. Comparing the SEM pictures of ZnO-NWs and Pd-ZnO-NWs shown in Figures 2(c) and 2(d), it is clear that the

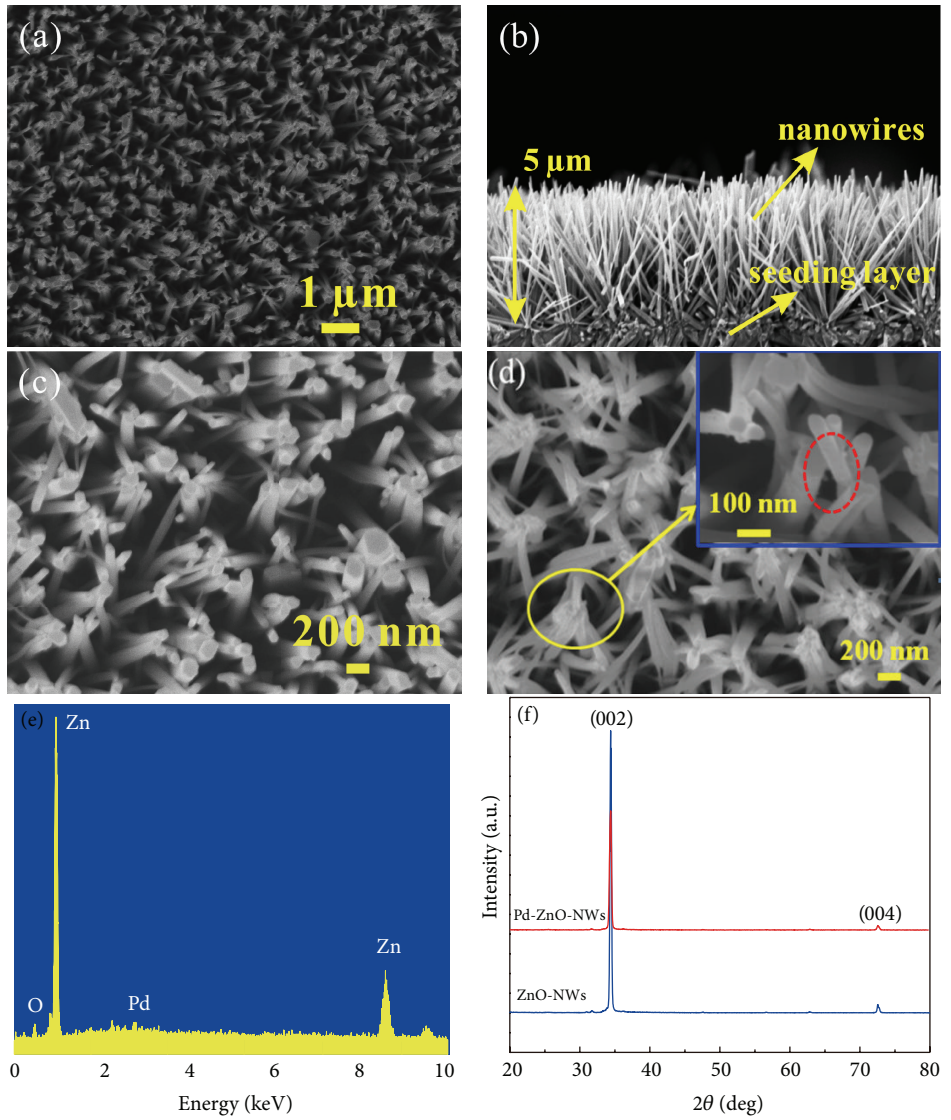

Figure 2: (a) Top-view and (b) side-view SEM images of ZnO-NWs grown on the substrate, (c) magnified top-view SEM images of ZnO-NWs and (d) Pd-ZnO-NWs (the inserted image shows the nanoparticles of Pd on ZnO-NWs), (e) EDS spectrum of Pd-ZnO-NWs, and (f) the XRD spectra of ZnO-NWs and Pd-ZnO-NWs.

morphology of ZnO-NWs remains unchanged after Pd decoration. However, the small particles on ZnO-NWs surface can be seen in the inserted image of Figure 2(d). The results of EDS analyses are shown in Figure 2(e), indicating that the sample of Pd-ZnO-NWs is indeed composed of Zn, O, and Pd. This demonstrates that Pd has been successfully decorated on the surface of ZnO-NWs.

To investigate the crystalline structures of ZnO-NWs and Pd-ZnO-NWs, XRD spectra of the samples are obtained as shown in Figure 2(f). The diffraction peaks in the XRD patterns are the same as the standard card (JCPDS 36-1451) with a wurtzite structure of ZnO by indexing. A strong and sharp peak located at (002) crystal plane of the prepared ZnO-NWs reveals their high quality crystallinity and *c*-axis orientation [27]. No diffraction peaks of Pd could be observed, however, in the XRD pattern of Pd-ZnO-NWs, due probably to the fact that the Pd content is much lower than that of Zn or O in Pd-ZnO-NWs [28, 29].

3.2. Gas Sensing Properties. In order to confirm a good gas selectivity of the sensors, we have performed sensing studies of ZnO-NWs and Pd-ZnO-NWs for various gases such as CH_4, CO, CH_3OH, CH_3COCH_3, and C_2H_5OH (Figure 3). The concentration of all the analytes is 200 ppm. Figure 3(a) shows that the ZnO-NWs sensor does not respond to CH_4 and CO gases in the whole range of testing temperatures. On the other hand, the same sensor shows the detectable signal with CH_3OH, CH_3COCH_3, and C_2H_5OH gases, indicating also a maximum response at a temperature of 425°C. The maximum sensitivities to CH_3COCH_3 and CH_3OH are found to be 1.68 and 1.30, respectively, which are much lower compared to that of C_2H_5OH (~2.69). The gas selectivity

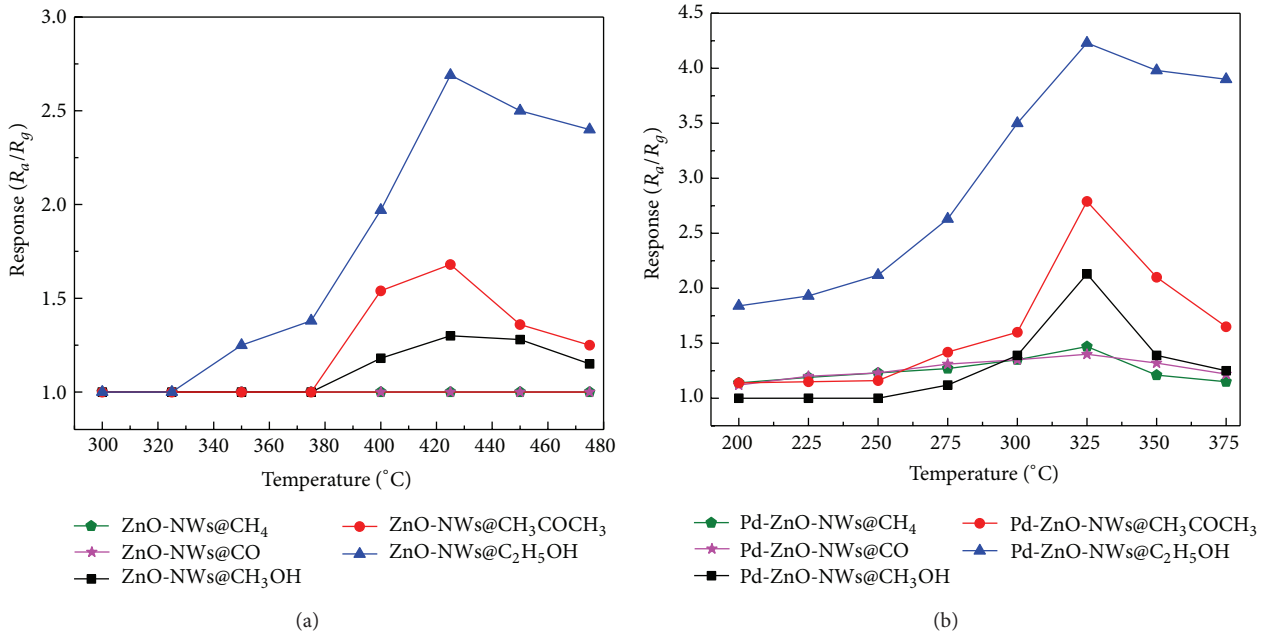

Figure 3: Response of (a) ZnO-NWs and (b) Pd-ZnO-NWs to different gases of 200 ppm concentration at various operating temperatures.

Table 1: Selectivity factor (Q) of the sensors fabricated by ZnO-NWs and Pd-ZnO-NWs. ($Q = S_{ethanol}/S_{other}$, where $S_{ethanol}$ and S_{other} are the responses of the sensors to 200 ppm ethanol and other gases, resp.).

	Target gases				
	C_2H_5OH	CH_4	CO	CH_3OH	CH_3COCH_3
Q factor of ZnO-NWs	1	2.69	2.69	2.07	1.60
Q factor of Pd-ZnO-NWs	1	2.88	3.02	1.99	1.52

experiments were also carried out with Pd-ZnO-NWs sensor (Figure 3(b)). The results show that the sensor is sensitive to all testing gases after Pd was decorated, and the maximum responses to different gases appear at the same temperature of 325°C, which is lower than that of ZnO-NWs. Now, the maximum sensitivities to C_2H_5OH, CH_3COCH_3, CH_3OH, CH_4, and CO are 4.23, 2.79, 2.13, 1.47, and 1.4, respectively.

To evaluate the gas selectivity of sensors, we define a selectivity factor (Q) as $Q = S_e/S_o$ [28], where S_e and S_o are the responses of the sensors to 200 ppm ethanol and 200 ppm of other gases in this work, respectively. The bigger the value of Q of a sensor, the higher the selectivity to the ethanol gas. From the results listed in Table 1, we can find that the two types of sensors have a better selectivity to ethanol at the ambient of CO or CH_4. Clearly, the sensing selectivity has been increased after Pd decoration.

To investigate the sensing properties of ZnO-NWs and Pd-ZnO-NWs for ethanol gas, the ZnO-NWs grown on the substrate were dipped in an ethanol solution of 9.6 mM palladium chloride and this process was repeated 3, 5, and 7 times, respectively. We refer to these samples as Pd-ZnO-NWs-3, Pd-ZnO-NWs-5, and Pd-ZnO-NWs-7, representing

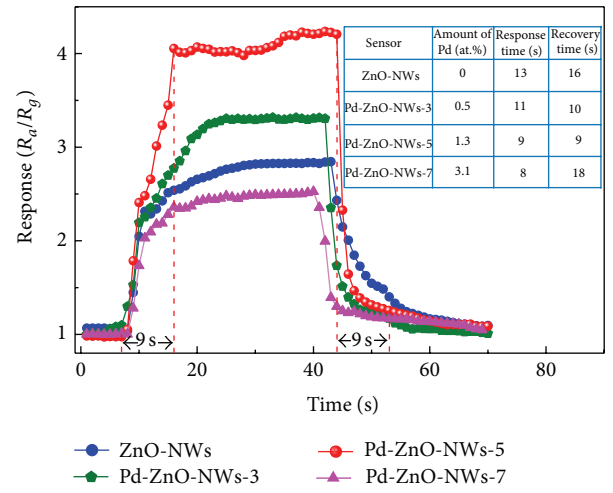

Sensor	Amount of Pd (at.%)	Response time (s)	Recovery time (s)
ZnO-NWs	0	13	16
Pd-ZnO-NWs-3	0.5	11	10
Pd-ZnO-NWs-5	1.3	9	9
Pd-ZnO-NWs-7	3.1	8	18

Figure 4: Transient responses of ZnO-NWs and Pd-ZnO-NWs-x (x = 3, 5, and 7) exposed to 200 ppm ethanol.

0.5%, 1.3%, and 3.1% atomic percentage of Pd on the surface of ZnO-NWs. Figure 4 shows the response value and response-recovery time of the ZnO-NWs and Pd-ZnO-NWs-x (x = 3, 5 and 7) sensors exposed to 200 ppm ethanol at their own optimum operating temperature of 425°C and 325°C. When the Pd concentration on the surface of samples is increased from 0.5 to 3.1 at. %, Pd-ZnO-NWs-5 shows an improved sensor performance in terms of response value (4.23) and response-recovery times (9 s and 9 s), which are better than those of ZnO-NWs and Pd-ZnO-NWs-3 as well as those of previously reported data (Table 2). A further increase of the Pd concentration leads to the increase of the recovery time and the deterioration of the sensitivity.

Table 2: The Comparison with the fabrication parameters of Pd-ZnO-NWs sensors reported in the literature and our work.

Structure	Diameter/length (nm/μm)	Concentration (ppm)	Operating temperature (°C)	Response[a] (%)	Response/recovery time (s)
Pd-ZnO-NWs-5 (our work)	70–100/5	200	325	76.4	9/9
Pd-decorated ZnO nanorods [22]	70/0.5	1530	200	94	14/70
Pd-sensitized ZnO-NWs [20]	50/3.5	500	230	61.5	a few seconds/more than 100 seconds
Pd-functionalized individual ZnO microwire [23]	1000/50–200	200	400	13	–/–
Pd/ZnO spheroidal and rod-like nanoparticles [24]	10–20 width: 10–20 length: 20–50	250	400	65.7	15/within minutes
Pd incorporated ZnO nanoparticles [20]	17	200	170	68	60/10

[a]Applies $(R_a - R_g)/R_a$ for the response.

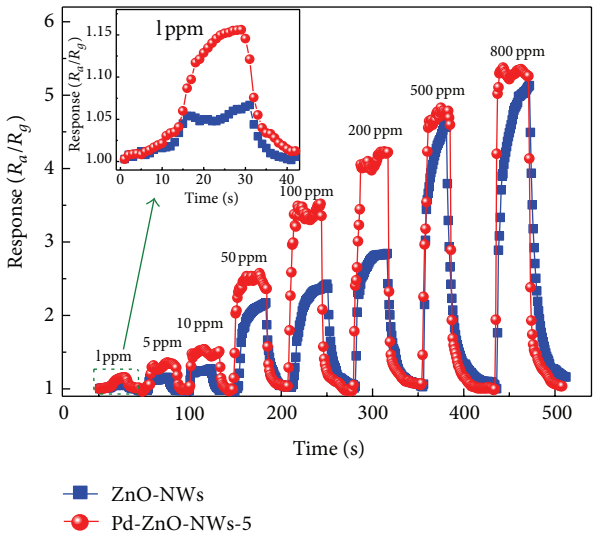

Figure 5: Dynamic responses of ZnO-NWs and Pd-ZnO-NWs-5 sensors to ethanol in the detection range from 1 to 800 ppm. The inserted image shows the partial magnified response curve of sensors exposed to 1 ppm ethanol.

Figure 5 shows the dynamic responses of ZnO-NWs and Pd-ZnO-NWs-5 exposed to different concentrations of ethanol at their optimum temperature, showing clearly a fast and repeatable response-recovery performance for ethanol. When the concentration of ethanol changes from 1 to 200 ppm, the response of Pd-ZnO-NWs-5 is higher than that of ZnO-NWs. When the concentration is larger than 500 ppm, however, the ZnO-NWs and Pd-ZnO-NWs-5 sensors show almost the same response. Remarkably, both sensors can detect ethanol of a concentration as low as 1 ppm, but Pd-ZnO-NWs-5 sensor shows a better performance (insert of Figure 5) than the ZnO-NWs, with a response and recovery time of 12 s and 10 s, respectively.

Figure 6(a) shows the response curves of two sensors at their optimum temperature as a function of ethanol concentration in the range of 1 to 800 ppm. Clearly, the response of Pd-ZnO-NWs-5 sensor increases faster than that of ZnO-NWs sensor. The Pd-ZnO-NWs-5 sensor also has a better linearity than that of ZnO-NWs up to 100 ppm, indicating that Pd-ZnO-NWs-5 sensor is more favorable to detect low concentration ethanol. When the concentration of ethanol is increased to 500 ppm, the responses of two sensors increase slowly, due presumably to the saturation of both sensors.

3.3. Mechanistic Understanding of Ethanol Sensing. It is well known that chemisorbed oxygen plays a key role in electrical transmission of semiconducting metal oxides [30, 31], and the sensitivity of the gas sensor depends on the interaction between chemisorbed oxygen and sensing materials. As reactive oxygen, chemisorbed oxygen can be divided into O_2^-, O^{2-}, and O^-. Empirically, the response of the sensor can be expressed as follows [31]:

$$\log(S-1) = \alpha \log C_{\text{gas}} + \log \beta, \tag{2}$$

where S is the response of sensor, C_{gas} is the concentration of target gas, α and β are constants, α is a value represents the species of oxygen ion on the surface of ZnO-NWs [32]. It was reported that for α of 0.5 the chemisorbed oxygen ion on the surface is O^{2-} and for α of 1, the chemisorbed oxygen ion is O^- [31]. Figure 6(b) shows the linear relationship between the sensor response and the ethanol concentration. The slopes of the two lines (0.61 and 0.52, resp.) are close to 0.5, which means that the dominated species of the oxygen ion on ZnO surface are O^{2-} ions. These oxygen ions can trap electrons from ZnO and form a space-charge region which makes the resistance of sensor increase. When the reducing gas (such as ethanol) is injected into the chamber, the ionic oxygen reacts with ethanol and produces CO_2 and H_2O and then releases a large number of electrons. These released electrons will go back to the conduction band, leading to the decrease of metal oxide resistance. The reaction process can be described as follows [33]:

$$O_2 + e^- \longrightarrow O_2^-$$

$$O_2^- + e^- \longrightarrow 2O^-$$

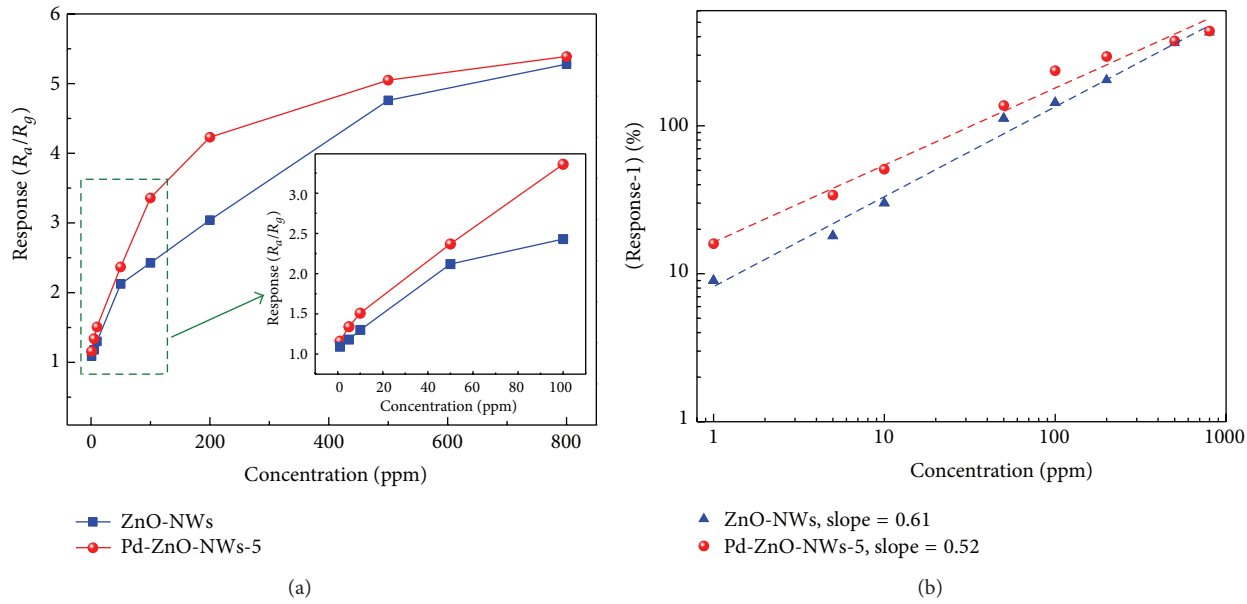

FIGURE 6: (a) Response of ZnO-NWs and Pd-ZnO-NWs-5 versus ethanol concentrations (the inserted image shows the partial magnified response curve of the two sensors exposed to 1–100 ppm ethanol), (b) linear relationship between log(Response-1) and log C_{gas}.

$$O^- + e^- \longrightarrow O^{2-}$$
$$C_2H_5OH + 6O^{2-} \longrightarrow 2CO_2 + 3H_2O + 12e^- \quad (3)$$

Our data have shown that the additive Pd can improve the gas sensing properties of the ZnO sensors to ethanol. At high temperature, oxygen molecules can weakly bond to the catalytic atoms Pd [34], and the oxygen atom is produced in a complex dissociation reaction (4) [35]. This oxygen atom finally becomes negatively charged oxygen ion by trapping an electron from the surface of ZnO (5).

Consider the following:

$$2Pd + O_2 \longrightarrow 2Pd : O \quad (4)$$
$$O + e^- \longrightarrow O^- \quad (5)$$

Meanwhile, because of the PdO attached on the surface of ZnO, a heterojunction at the interface between ZnO (n-type semiconductor) and PdO (p-type semiconductor) will be formed as shown in Figure 7(a). The heterojunction leads to the band bending in the depletion layers [36]. The electrons transfer from n-type ZnO to p-type PdO, whereas the holes transfer from PdO to ZnO until the system reaches the equilibrium state. These charge transfers will lead to a wider depletion layer and a greater resistance. As the reaction processing, the electrons will pass through the depletion layers of heterojunction under the certain high temperature, which makes the depletion layer at the PdO/ZnO interface once again become thin, facilitating the larger amount of electron transport between the PdO and ZnO, and as a result, the response-recovery times and optimum operating temperature of the sensor decrease significantly compared to its undecorated counterpart [22, 24].

Simultaneously, ethanol molecule can also combine with the hole in PdO (6) and produce the intermediates, which will react with the O^{2-} on the n-type ZnO (7) and release more electrons. Such catalytic dissociation of ethanol on Pd nanoparticles lowers the activation energy, enhances the reaction velocity, and improves the performance of the sensor as a whole. The schematic model of the ZnO-NWs and Pd-ZnO-NWs sensors when exposed to ethanol gas is shown in Figure 7(b).

Consider the following:

$$C_2H_5OH + h^+ \longrightarrow CH_3CH_2O + H^+ \quad (6)$$
$$CH_3CH_2O + H^+ + 6O^{2-} \longrightarrow 2CO_2 + 3H_2O + 11e^- \quad (7)$$

4. Conclusion

ZnO-NWs were prepared by hydrothermal growth, showing high quality crystallinity and *c*-axis orientation. They were then used for gas sensing with or without Pd-decoration. Our results showed that the ZnO-NWs and Pd-ZnO-NWs were more selective to ethanol in the presence of CH_4, CO, CH_3OH, and CH_3COCH_3. Comparing to the as-grown ZnO-NWs, Pd-ZnO-NWs showed a higher sensitivity, faster response, higher selectivity, and lower operating temperature. Typically, the response of Pd-ZnO-NWs was 57% higher and the optimum operating temperature was 100°C lower than those of ZnO-NWs. When exposed to 200 ppm ethanol, the response and recovery time (both 9 s) of Pd-ZnO-NWs-5 were shorter than those of pure ZnO-NWs (13 s and 16 s, resp.). These improvements could be attributed to the formation of the heterojunction between PdO and ZnO. We believe that the Pd-ZnO-NWs hold a great potential for high-performance detection of ethanol gas.

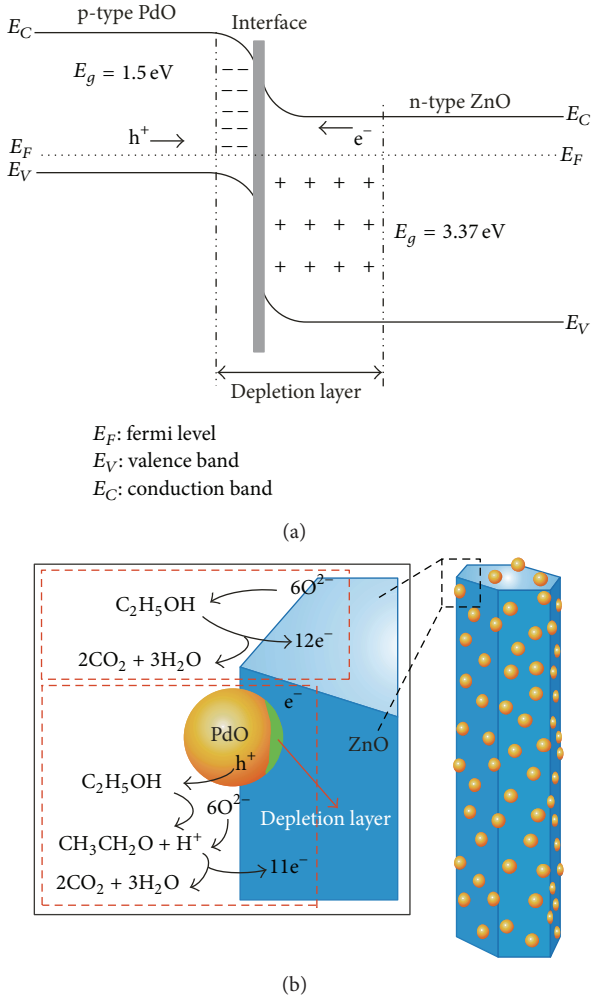

FIGURE 7: (a) Diagram of energy band structure for p-type PdO/n-type ZnO heterojunction, (b) schematic model of the ZnO-NWs and Pd-ZnO-NWs sensors exposed to ethanol gas.

Acknowledgments

The authors thank the National Natural Science Foundation of China (Grant nos. 51205273 and 51205274), the Shanxi Province Science Foundation for Youths (Grant no. 2013021017-2), the Scientific and Technological Innovation Programs of Higher Education Institutions in Shanxi (Grant no. 20120007), the Shanxi Scholarship Council of China (Grant no. 2013-035), the Excellent Innovation Programs for Postgraduate in Shanxi Province (Grant no. 20133028), the Special/Youth Foundation of Taiyuan University of Technology (Grant nos. 2012L034 and 2012L011), and also the Excellent Graduate's Science and Technology Innovation Foundation of Taiyuan University of Technology (Grant no. 2013A005).

References

[1] G. Eranna, B. C. Joshi, D. P. Runthala, and R. P. Gupta, "Oxide materials for development of integrated gas sensors—a comprehensive review," *Critical Reviews in Solid State and Materials Sciences*, vol. 29, no. 3-4, pp. 111–188, 2004.

[2] H.-W. Ryu, B.-S. Park, S. A. Akbar et al., "ZnO sol-gel derived porous film for CO gas sensing," *Sensors and Actuators B*, vol. 96, no. 3, pp. 717–722, 2003.

[3] J. X. Wang, X. W. Sun, A. Wei et al., "Zinc oxide nanocomb biosensor for glucose detection," *Applied Physics Letters*, vol. 88, no. 23, Article ID 233106, 2006.

[4] N. Al-Hardan, M. J. Abdullah, and A. A. Aziz, "The gas response enhancement from ZnO film for H_2 gas detection," *Applied Surface Science*, vol. 255, no. 17, pp. 7794–7797, 2009.

[5] E. Hosono, S. Fujihara, I. Honma, and H. Zhou, "The fabrication of an upright-standing zinc oxide nanosheet for use in dye-sensitized solar cells," *Advanced Materials*, vol. 17, no. 17, pp. 2091–2094, 2005.

[6] W. I. Park, J. S. Kim, G.-C. Yi, M. H. Bae, and H.-J. Lee, "Fabrication and electrical characteristics of high-performance ZnO nanorod field-effect transistors," *Applied Physics Letters*, vol. 85, no. 21, pp. 5052–5054, 2004.

[7] S. Liang, H. Sheng, Y. Liu, Z. Huo, Y. Lu, and H. Shen, "ZnO Schottky ultraviolet photodetectors," *Journal of Crystal Growth*, vol. 225, no. 2–4, pp. 110–113, 2001.

[8] Z. T. Han, S. S. Li, J. K. Chu, and Y. Chen, "Electrospun Pd-doped ZnO nanofibers for enhanced photocatalytic degradation of methylene blue," *Journal of Sol-Gel Science and Technology*, vol. 66, no. 1, pp. 139–144, 2013.

[9] D. Mishra, A. Srivastava, A. Srivastava, and R. K. Shukla, "Bead structured nanocrystalline ZnO thin films: synthesis and LPG sensing properties," *Applied Surface Science*, vol. 255, no. 5, pp. 2947–2950, 2008.

[10] K. J. Chen, F. Y. Hung, S. J. Chang, and S. J. Young, "Opto-electronic characteristics of UV photodetector based on ZnO nanowire thin films," *Journal of Alloys and Compounds*, vol. 479, no. 1-2, pp. 674–677, 2009.

[11] P. Bhattacharyya, P. K. Basu, H. Saha, and S. Basu, "Fast response methane sensor using nanocrystalline zinc oxide thin films derived by sol-gel method," *Sensors and Actuators B*, vol. 124, no. 1, pp. 62–67, 2007.

[12] C. S. Prajapati and P. P. Sahay, "Alcohol-sensing characteristics of spray deposited ZnO nano-particle thin films," *Sensors and Actuators B*, vol. 160, no. 1, pp. 1043–1049, 2011.

[13] T.-J. Hsueh, Y.-W. Chen, S.-J. Chang et al., "ZnO nanowire-based CO sensors prepared on patterned ZnO:Ga/SiO2/Si templates," *Sensors and Actuators B*, vol. 125, no. 2, pp. 498–503, 2007.

[14] H. Zhang, D. Yang, D. Li, X. Ma, S. Li, and D. Que, "Controllable growth of ZnO microcrystals by a capping-molecule-assisted hydrothermal process," *Crystal Growth and Design*, vol. 5, no. 2, pp. 547–550, 2005.

[15] X. Jiaqiang, C. Yuping, C. Daoyong, and S. Jianian, "Hydrothermal synthesis and gas sensing characters of ZnO nanorods," *Sensors and Actuators B*, vol. 113, no. 1, pp. 526–531, 2006.

[16] N. Hongsith, C. Viriyaworasakul, P. Mangkorntong, N. Mangkorntong, and S. Choopun, "Ethanol sensor based on ZnO and Au-doped ZnO nanowires," *Ceramics International*, vol. 34, no. 4, pp. 823–826, 2008.

[17] F.-C. Huang, Y.-Y. Chen, and T.-T. Wu, "A room temperature surface acoustic wave hydrogen sensor with Pt coated ZnO nanorods," *Nanotechnology*, vol. 20, no. 6, Article ID 065501, 2009.

[18] P. Mitra and H. S. Maiti, "A wet-chemical process to form palladium oxide sensitiser layer on thin film zinc oxide based LPG sensor," *Sensors and Actuators B*, vol. 97, no. 1, pp. 49–58, 2004.

[19] Q. Xiang, G. Meng, Y. Zhang et al., "Ag nanoparticle embedded-ZnO nanorods synthesized via a photochemical method and its gas-sensing properties," *Sensors and Actuators B*, vol. 143, no. 2, pp. 635–640, 2010.

[20] B. Baruwati, D. K. Kumar, and S. V. Manorama, "Hydrothermal synthesis of highly crystalline ZnO nanoparticles: a competitive sensor for LPG and EtOH," *Sensors and Actuators B*, vol. 119, no. 2, pp. 676–682, 2006.

[21] T.-J. Hsueh, S.-J. Chang, C.-L. Hsu, Y.-R. Lin, and I.-C. Chen, "Highly sensitive ZnO nanowire ethanol sensor with Pd adsorption," *Applied Physics Letters*, vol. 91, no. 5, Article ID 053111, 2007.

[22] S. Roy, N. Banerjee, C. Sarkar, and P. Bhattacharyya, "Development of an ethanol sensor based on CBD grown ZnO nanorods," *Solid-State Electronics*, vol. 87, pp. 43–50, 2013.

[23] G. Y. Chai, O. Lupan, E. V. Rusu et al., "Functionalized individual ZnO microwire for natural gas detection," *Sensors and Actuators A*, vol. 176, pp. 64–71, 2012.

[24] C. Liewhiran, A. R. Camenzind, A. Teleki, S. E. Pratsinis, and S. Phanichphant, "Doctor-bladed thick films of flame-made Pd/ZnO nanoparticles for ethanol sensing," *Current Applied Physics*, vol. 8, no. 3-4, pp. 336–339, 2008.

[25] J.-H. Tian, J. Hu, S.-S. Li et al., "Improved seedless hydrothermal synthesis of dense and ultralong ZnO nanowires," *Nanotechnology*, vol. 22, no. 24, Article ID 245601, 2011.

[26] X. Li, Y. Chang, and Y. Long, "Influence of Sn doping on ZnO sensing properties for ethanol and acetone," *Materials Science and Engineering C*, vol. 32, no. 4, pp. 817–821, 2012.

[27] Y.-H. Hsu, J. Lin, and W. C. Tang, "RF sputtered piezoelectric zinc oxide thin film for transducer applications," *Journal of Materials Science: Materials in Electronics*, vol. 19, no. 7, pp. 653–661, 2008.

[28] M. Zhao, X. Wang, J. Cheng, L. Zhang, J. Jia, and X. Li, "Synthesis and ethanol sensing properties of Al-doped ZnO nanofibers," *Current Applied Physics*, vol. 13, no. 2, pp. 403–407, 2012.

[29] Y. Zeng, Z. Lou, L. Wang et al., "Enhanced ammonia sensing performances of Pd-sensitized flowerlike ZnO nanostructure," *Sensors and Actuators B*, vol. 156, no. 1, pp. 395–400, 2011.

[30] W. Zeng, T. Liu, and Z. Wang, "Impact of Nb doping on gas-sensing performance of TiO_2 thick-film sensors," *Sensors and Actuators B*, vol. 166-167, pp. 141–149, 2012.

[31] S. Choopun, A. Tubtimtae, T. Santhaveesuk, S. Nilphai, E. Wongrat, and N. Hongsith, "Zinc oxide nanostructures for applications as ethanol sensors and dye-sensitized solar cells," *Applied Surface Science*, vol. 256, no. 4, pp. 998–1002, 2009.

[32] Y. H. Shi, M. Q. Wang, C. Hong et al., "Multi-junction joints network self-assembled with converging ZnO nanowires as multi-barrier gas sensor," *Sensors and Actuators B*, vol. 177, pp. 1027–1034, 2012.

[33] P. P. Sahay, "Zinc oxide thin film gas sensor for detection of acetone," *Journal of Materials Science*, vol. 40, no. 16, pp. 4383–4385, 2005.

[34] K. V. Gurav, P. R. Deshmukh, and C. D. Lokhande, "LPG sensing properties of Pd-sensitized vertically aligned ZnO nanorods," *Sensors and Actuators B*, vol. 151, no. 2, pp. 365–369, 2011.

[35] V. R. Shinde, T. P. Gujar, and C. D. Lokhande, "Enhanced response of porous ZnO nanobeads towards LPG: effect of Pd sensitization," *Sensors and Actuators B*, vol. 123, no. 2, pp. 701–706, 2007.

[36] G. Eranna, B. C. Joshi, D. P. Runthala, and R. P. Gupta, "Oxide materials for development of integrated gas sensors-a comprehensive review," *Critical Reviews in Solid State and Materials Sciences*, vol. 29, no. 3-4, pp. 111–188, 2004.